ACS OMEGA

http://pubs.acs.org/journal/acsodf

Article

Chemical Kinetic Modeling of Air−Steam Gasification of Eucalyptus Wood Sawdust for H_2-Rich Syngas Production

Ajay Sharma* and Ratnadeep Nath

Cite This: *ACS Omega* 2023, 8, 13396−13409

Read Online

ACCESS | Metrics & More | Article Recommendations

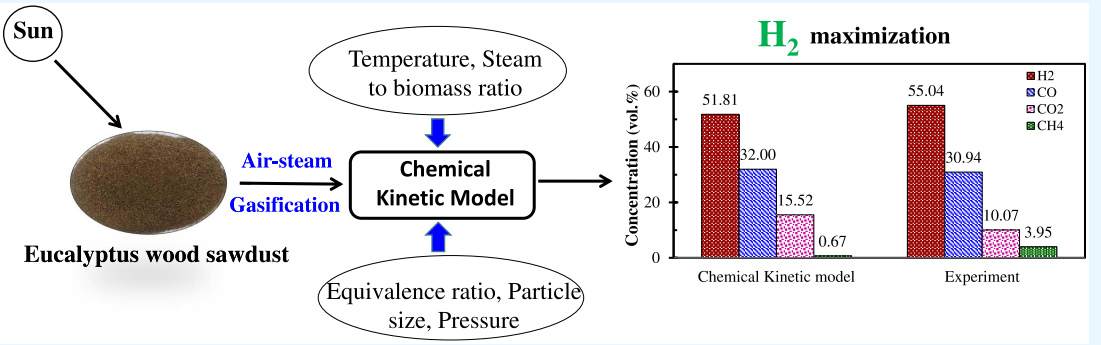

ABSTRACT: The aim of this research paper is to develop a chemical kinetic model, based on the mechanism of surface reactions, for air−steam gasification of eucalyptus wood sawdust ($CH_{1.63}O_{1.02}$) and analyze the hydrogen-rich syngas production. Experiments are performed on a bubbling fluidized-bed gasifier using air−steam as a gasifying agent. For validation of the developed kinetic model, the outcome of the model is compared with that of experimental data, which shows a root-mean-square error of less than 4. Different parameters such as equivalence ratios ($0 \le ER \le 0.4$), particle size ($100 \le Dp \le 1000$ μm), gasification temperature ($900 \le T \le 1200$ K), pressure ($1 \le P \le 20$ atm), and steam-to-biomass ratio ($0 \le SBR \le 2$) are considered for the analysis. The one-parameter-at-a-time concept is employed to maximize the production of H_2-rich syngas. Results indicate that the maximum concentration of hydrogen is 55.04 vol % (experimental) and 51.81 vol % (predicted) at optimum conditions: ER = 0, Dp = 100 μm, T = 1100 K, P = 1 atm, and SBR = 0.75. Gasification performance parameters such as hydrogen gas yield, heating values, cold gas efficiency, etc., are evaluated.

1. INTRODUCTION

The most special characteristic of hydrogen energy is that when burned, it leaves no trace or residue affecting nature and human life, what it leaves behind is only water. Hence, hydrogen is recognized as the purest form of energy fuel. Scientists have made continuous efforts to change the global energy system toward fully green technology. Hydrogen, the lightest element (m.wt. = 1 g/mol), is a zero-emission fuel, having the characteristics of the highest energy density, high inflammability, and explosiveness when it comes in contact with oxygen. The energy density of hydrogen is 122 MJ/kg, which is about 2.75 times higher than that of gasoline. It is believed that hydrogen would be an effective alternative to gasoline in the near future. Therefore, developing countries are focusing on H_2 energy, a fully green technology [$H_2(g) + O_2(g) = H_2O(l) +$ energy]. Recently, in March 2020, the world's largest plant for hydrogen gas production was opened in Fukushima, Japan. The systems available for power generation using hydrogen include fuel cells,[1] nuclear conversion,[2] supercritical water gasification,[3,4] and thermo-chemical conversion,[5] among which thermal conversion has received the maximum attention from the scientific community.[5−9] Soria et al.[10] conducted an experimental study to determine the combined effect of pallet size, temperature, and heating rate on product gas compositions using the high-temperature fast pyrolysis process. However, for H_2 gas production, gasification is preferred over other thermochemical processes because almost all of the products of gasification are gases with a small amount of tar. Biomass is the third preferable source after coal and oil for power generation. It does not add greenhouse gases to the atmosphere as it has the property of absorbing the same amount of carbon as it releases. It is renewable, abundantly available, and accessible. Apart

Received: February 11, 2023
Accepted: March 21, 2023
Published: March 31, 2023

from its advantages of accessibility, renewability, and abundant availability, it can be used in thermal power generation plants (using fossil fuels) without much changes to the plant equipment/machinery.

Gasification converts organic or fossil-based carbonaceous materials into a combustible gaseous mixture (mainly CO, H_2, CO_2, and CH_4). This fuel conversion takes place at an elevated temperature (≥600 °C) in the presence of insufficient gasifying agents (air, O_2, H_2O(g), and CO_2) with a concomitant range of calorific values (CVs): low (4−6 MJ/Nm^3), medium (10−16 MJ/Nm^3), and high (40 MJ/Nm^3).[11] Among all, steam is preferred over other gasifying agents as it improves the combustible quality of syngas through the addition of H_2(g) by accelerating the steam gasification, methane reformation, and water−gas shift reaction. Based on the system operation, gasifiers are classified into three types, including fixed bed, fluidized bed, and entrained bed. Fluidized-bed gasifiers are favored among the three due to the advantages of tar reduction, good solid−gas contact, good heat and mass transport, fuel flexibility, easy char separation, low pressure drop, and good control of temperature.[11] Rodriguez et al.[12] executed an experimental and theoretical analysis of lignocellulosic winery wastes using a fluidized-bed gasifier. Apart from the basic technology and design aspects of gasifiers, there are other factors that influence the yield of H_2 in steam gasification. Some of the prominent factors are the type, quality, inherent moisture content, particle size, and density of the feedstock, reaction temperature, bed height, heating rate, environment, flow of medium, steam flow rate, addition of catalyst, and sorbent-to-biomass ratio.[11,13,14]

Different studies have been reported[5,6,15,16] dealing with the influence of process parameters such as reaction temperature, gasifying agents, various catalysts with their loading, and sorbent-to-biomass ratio. Most of the studies were based on the Gibbs free energy minimization method[5,17,18] rather than the stoichiometry-based model. However, because of the accuracy, robustness, and reliability, researchers prefer the stoichiometry-based model.[19,20] The Wang and Kinoshita model[21] is referred to as the beginning of the kinetic modeling of biomass gasification using the Langmuir−Hinshelwood mechanism. Parameters such as the residence time, type of oxidant, char particle size, temperature, pressure, and equivalence ratio are considered, and their impacts on the product gas composition and conversion ratio are investigated. Recently, a thermodynamic approach based on the Gibbs free energy minimization method was utilized by Echegaray et al.[22] when performing an exergy analysis for air−steam gasification with lignocellulosic waste as a feedstock material. While modeling, the water−gas shift reaction was involved in the reactions. Using eucalyptus and pine residue, Puig-Gamero et al.[23] conducted both simulation (kinetic modeling) and experimental studies on a bubbling fluidized-bed gas reactor. The authors focused on H_2 and tar production/prediction and discussed their behavior with the equivalence ratio, temperature, and particle size. Torres-Sciancalepore et al.[24] performed a thermogravimetry-based kinetic modeling and product analysis to obtain the pyrolysis kinetic parameters and output gas composition of sweet briar rosehip seed waste. It was concluded that the highest production of H_2 and CH_4 occurred between 350 and 400 °C and that of CO_2 and CO occurred between 300 and 350 °C. Moreover, Fernandez et al.[25] performed steam-assisted kinetic modeling for the gasification of three different agroindustrial solid wastes using the micro TGA technique. They found that the overall process is governed by a first-order model for devolatilization and the Ginstling−Brounstein diffusion model for char gasification. A numerical analysis of biomass gasification was carried out by Song et al.[26] for H_2-rich syngas production using a process simulator like Aspen Plus. Results showed that H_2 production increases with an increase in the temperature (750−900 °C), steam-to-biomass ratio (0.25−1.0), and equivalence ratio (0.1−0.4). Champion et al.[27] developed a chemical kinetic model to understand the effect of temperature and equivalence ratio on syngas compositions. The model assumed that the plug flow pattern of product gases released from the bed is approximately the same as the output of 10 CSTRs in series. It is concluded that temperatures from 950 to 1050 K and equivalence ratios from 0.25 to 0.35 have a significant impact on hydrogen-rich syngas production. An Aspen Plus gasification model based on the "Peng−Robinson/Boston−Mathias (PR-BM) equation of state" was studied by Cao et al.[28] using pine sawdust as a feedstock material. Changes in the gas composition, gas yield, tar yield, and higher heating values are examined with the variation in ER and SBR. The authors reported that with an increase in the ER value from 0.21 to 0.23, there is a diminishing trend for CO and CH_4 gas components, whereas SBR is a crucial parameter for the gasifier performance.

From the above literature review, it has been observed that most of the research studies employ commercial tools for the chemical kinetic modeling of biomass gasification, where the Gibbs free minimization model is used through a robust, accurate, and reliable mechanism such as the Langmuir−Hinshelwood mechanism, which is based on the kinetic theory of gases. Moreover, hardly any research work is available on the kinetic modeling of feedstock materials such as eucalyptus wood sawdust. This knowledge gap motivates the authors to consider eucalyptus wood sawdust for kinetic modeling and examine the influence of operating parameters on H_2-rich syngas production. Such analyses are important to understand the practical usability of the eucalyptus wood sawdust. The current research work extends the Wang and Kinoshita kinetic model[21] by incorporating the water−gas shift reaction in the analysis. An experimental work has also been conducted in a lab-scale bubbling fluidized-bed gasifier (BFBG) in order to validate the results obtained from the present kinetic model with the experimental data. Variations of the product gas composition with five operating parameters such as temperature, particle size, pressure, equivalence ratio, and steam-to-biomass ratio are discussed. Moreover, the hydrogen gas concentration, hydrogen and synthesis gas yield, heating values, cold gas efficiency of product gas, carbon conversion, and gasification efficiency are also computed. By analyzing all of the results for the variation of different operating parameters, the optimum conditions are reported for maximizing H_2-rich syngas production.

2. MATERIALS AND METHODS

2.1. Material Collection and Preparation. The eucalyptus wood sawdust (EWS) is collected as waste from a sawmill at Meerut, Uttar Pradesh (India). The sample was ground to obtain an average particle size of 100 and 1000 μm. In order to avoid heat- and mass-transfer limitations, small-sized particles (≤1000 μm) are considered for gasification purposes.[29,30] The sieved sample is kept in a closed plastic zip-bag to minimize moisture absorption from the surrounding

https://doi.org/10.1021/acsomega.3c00908
ACS Omega 2023, 8, 13396−13409

humidity. As per the observation of Geldart for the classification of sand particle fluidization, particles with sizes in the range of 150−500 μm and a density of 1.4−4 g/cm^3 (Geldart B) will be considered as the best suitable for the fluidization process.[31] In this research work, the sand particle size is taken as 350 μm and density as 2.61 g/cm^3, which is well within the Geldart classification, resulting in vigorous bubbling fluidization. Bubbles form as soon as the velocity exceeds the minimum fluidization velocity. The majority of the gas−solid reactions occur in this regime based on the particle size of raw materials.

2.2. Feedstock Characterization. The proximate analysis was performed as per the American Society for Testing and Materials (ASTM) standards [proximate; volatile content ASTM E872, moisture ASTM E871, ash ASTM D1102, and fixed carbon (by difference)]. The detailed procedure has been discussed in an earlier study.[32] A CHNS/O analyzer (Perkin Elmer 2400) was used to determine the elemental composition of EWS biomass. The elemental composition of materials mainly includes the wt % of carbon, hydrogen, nitrogen, and sulfur. The wt % of oxygen was determined by subtracting the wt % of C, H, N, and S from a total of 100. Finally, the higher and lower heating values (HHV and LHV) of EWS biomass were computed using analytical expressions given by Channiwala and Parikh.[33,34]

2.3. Description of the Kinetic Model. The development of a kinetic model for biomass gasification is challenging due to the high variation in the feedstock material and its structural behavior. Using the Langmuir−Hinshelwood mechanism, Wang and Kinoshita[21] proposed a kinetic model where reaction rates are developed that involve the formulation of differential equations for the syngas and char composition. Because of enormous reaction attempts in surface catalytic reactions,[35] such a model is preferred and widely accepted. The present study is an extension of this kinetic model where an additional equation (like water-gas shift reaction) is considered in order to calculate gas compositions close to the actual chemical reactions.

A general equation for the air−steam gasification of biomass in a gasifier is given below:

Air−steam gasification of sawdust on a 1 mol basis[21]

$$CH_\alpha O_\beta + yO_2 + zN_2 + wH_2O \rightarrow x_1C + x_2H_2 + x_3CO + x_4H_2O + x_5CO_2 + x_6CH_4 + x_7N_2(\Delta H = +ve) \quad (1)$$

where, for eucalyptus wood, α = 1.63 and β = 1.02; x_1, x_2, x_3, x_4, x_5, x_6, and x_7 are the moles of char, H_2, CO, H_2O, CO_2, CH_4, and N_2, respectively.

The present analysis investigates within the temperature range of 900−1200 K; here, sawdust reacts with a mixture of air and superheated steam and converts into char and a gaseous mixture (H_2, CO, CO_2, and CH_4). This reaction is irreversible at each temperature and always promotes H_2 gas production. The following reactions occurred during the gasification process:

Char gasification

$$\text{Boudouard reaction}(R_1): C + CO_2 \leftrightarrow 2CO \quad (2)$$

$$\text{steam gasification}(R_2): C + H_2O \leftrightarrow CO + H_2 \quad (3)$$

$$\text{hydrogen gasification}(R_3): C + 2H_2 \leftrightarrow CH_4 \quad (4)$$

Homogeneous volatile reactions

$$\text{methane} - \text{steam reforming(MSR)}(R_4): CH_4 + H_2O \leftrightarrow CO + 3H_2 \quad (5)$$

$$\text{water} - \text{gas shift(WGS)}(R_5): CO + H_2O \leftrightarrow CO_2 + H_2 \quad (6)$$

Satisfying the continuity equation, the following equations are solved at t = 0:

$$x_2 = x_3 = 0; \quad x_7 = z$$

$$\text{carbon balance: } x_1 + x_5 + x_6 = 1 \quad (7)$$

$$\text{hydrogen balance: } 2x_4 + 4x_6 = \alpha + 2w \quad (8)$$

$$\text{oxygen balance: } x_4 + 2x_5 = 2y + \beta + w \quad (9)$$

$$\text{steam balance: } x_4 = \mu x_5 + w \quad (10)$$

where μ represents the ratio of steam to carbon dioxide. In the present research work, μ = 1 is considered throughout the analysis[21] assuming that equal amounts of CO_2 and H_2O steam are generated in the reaction zone.

Based on the Langmuir−Hinshelwood mechanism, the rate equation can be expressed as below[21]

For the Boudouard reaction (R_1)

$$-v_1 = \frac{k_1K_5C_T(p_5 - p_3^2/k_{p1})}{1 + \sum K_ip_i} \quad (11)$$

where v_i is the net reaction rate for the ith reaction, K_i is the adsorption constant for the ith gas species, k_{p1} is the equilibrium constant for the 1st reaction (i.e., R_1), and p_i is the partial pressure of the ith gas species, calculated as follows[21]

$$p_i = \frac{x_i}{P_X} \text{ where } P_X = \frac{1}{p}\sum_{i=2}^{7} x_i \quad (12)$$

Therefore, $p_3 = \frac{x_3}{P_X}$ and $p_5 = \frac{x_5}{P_X}$, and using $C_T = \frac{72k_s}{\rho d_p}\left(\frac{x_1(t=0)}{x_1}\right)^{1/3} x_1$, it can be written as follows[21]

$$-v_1 = \frac{k_1K_5C_T(x_5 - x_3^2/P_Xk_{p1})}{P_X\left(1 + \sum K_ip_i\right)} = \frac{k_1K_5C_T(x_5 - x_3/P_Xk_{p1})}{\left(P_X + \sum K_ip_iP_X\right)} = \frac{k_1K_5C_T(x_5 - x_3/P_Xk_{p1})}{\left(\sum \frac{1}{p}x_i + \sum K_ix_i\right)} - v_1 = k_{a1}\frac{(x_5 - x_3/P_Xk_{p1})}{\sum\left(K_i + \frac{1}{p}\right)x_i}\left(\frac{x_1}{\rho d_p}\right)\left(\frac{x_1(t=0)}{x_1}\right)^{1/3} \quad (13)$$

where $k_{a1} = 72k_sk_1K_5$ represents the rate constant (apparent), and k_{pi} is the equilibrium constant for the ith reaction. The values of the apparent rate constant and equilibrium rate constants are collected from HSC Chemistry (version 9.3.0) software and are listed in Table 2. The adsorption constants values are taken from available scientific reports.[36,37]

Similarly, for steam gasification (R_2)

https://doi.org/10.1021/acsomega.3c00908
ACS Omega 2023, 8, 13396−13409

$$-v_2 = k_{a2}\frac{(x_4 - x_3x_2/P_Xk_{p2})}{\sum\left(K_i + \frac{1}{p}\right)x_i}\left(\frac{x_1}{\rho d_p}\right)\left(\frac{x_1(t=0)}{x_1}\right)^{1/3} \quad (14)$$

Hydrogen gasification (R_3)

$$-v_3 = k_{a3}\frac{(x_2^2 - x_6P_X/k_{p3})}{P_X\sum\left(K_i + \frac{1}{p}\right)x_i}\left(\frac{x_1}{\rho d_p}\right)\left(\frac{x_1(t=0)}{x_1}\right)^{1/3} \quad (15)$$

Methane−steam reforming (MSR) (R_4)

$$-v_4 = k_{a4}\frac{(x_4x_6 - x_3x_2^3/P_X{}^2k_{p4})}{P_X\sum\left(K_i + \frac{1}{p}\right)x_i}\left(\frac{x_1}{\rho d_p}\right)\left(\frac{x_1(t=0)}{x_1}\right)^{1/3} \quad (16)$$

Water−gas shift (WGS) (R_5)

$$-v_5 = k_{a5}\frac{(x_3x_4 - x_5x_2/k_{p5})}{P_X\sum\left(K_i + \frac{1}{p}\right)x_i}\left(\frac{x_1}{\rho d_p}\right)\left(\frac{x_1(t=0)}{x_1}\right)^{1/3} \quad (17)$$

In order to calculate the gas composition and carbon content, the following differential equations must be solved

$$\frac{dx_1}{dt} = v_1 + v_2 + v_3 \quad (18)$$

$$\frac{dx_2}{dt} = -v_2 + 2v_3 - 3v_4 - v_5 \quad (19)$$

$$\frac{dx_3}{dt} = -2v_1 - v_2 - v_4 + v_5 \quad (20)$$

$$\frac{dx_4}{dt} = v_2 + v_4 + v_5 \quad (21)$$

$$\frac{dx_5}{dt} = v_1 - v_5 \quad (22)$$

$$\frac{dx_6}{dt} = -v_3 + v_4 \quad (23)$$

The above differential equations are numerically solved using an explicit method where initial guesses are obtained from eqs 18−23. A general formulation can be written as follows

$$\frac{X^{n+1} - x^n}{\Delta t} = f(\Phi^n) \quad (24)$$

where X is the gas/carbon content, Φ is the rate of reactions, $n + 1$ and n are the current and previous time levels, respectively, and Δt is the time level. An in-house-built FORTRAN code has been developed to obtain the gas composition by solving the aforesaid governing equations. The above equations are solved until a steady-state condition is achieved where the error is kept fixed at 1% between two successive time steps. To visualize the solution procedure in simple steps, a logic diagram is shown in Figure 1.

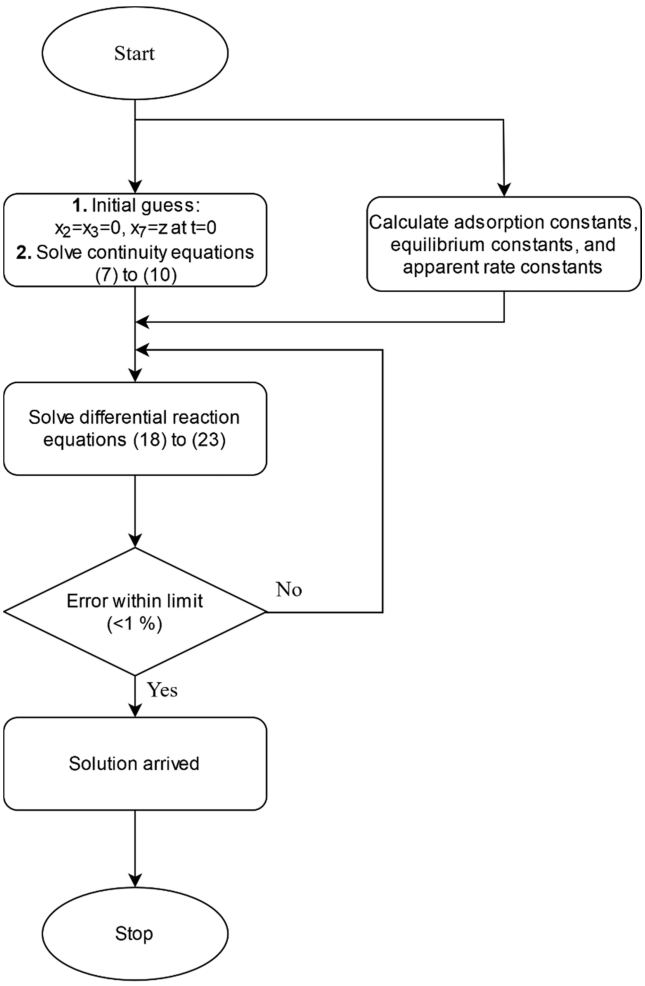

Figure 1. Logic diagram for the computation of the kinetic model of biomass gasification.

2.4. Description of the Experimental Setup. *2.4.1. Details of the Biomass Gasifier.* Apart from the chemical kinetic modeling, experiments are performed on the lab scale in order to confirm the validity of the data obtained by simulation. A bubbling fluidized-bed gasifier (BFBG) setup at the Process Engineering Research Laboratory of the Chemical Engineering Department at the Indian Institute of Technology Roorkee[17] has been used in this study, as shown in Figure 2a. The process of biomass gasification carried out in the gasifier is represented as a flow chart in Figure 2b. The components of the gasifier consist of a steam generator (Sg), a flow straightener with a ceramic porous disk, a reactor (R), split ceramic band heaters with an insulation jacket, a cyclone separator (C), a glass coil condenser (Gc), a water tank (W), a moisture trap (M), a gas flow meter with a totalizer, an inline flame arrestor, a chiller unit (Wc), a gas burner, and other auxiliaries such as thermocouples, PID controllers, gaskets, rupture disks, etc. The detailed specifications and limitations, and design purpose of each individual unit, are described in Table 1.

2.4.2. Experimental Procedure. With reference to Figure 2b, the following procedure has been adopted to perform the experimental run:

Approximately 2.5 kg of Fontainebleau sand having an average particle size of ∼350 μm ("−450 to +255") is placed inside the reactor (R) using valve "V_4" and then the valve is closed. Fifteen liters of distilled water is filled into the steam generator (Sg) through the H_2O feed line valve "V_1"; after ensuring that the water level is up to the mark, the valve "V_1" is closed. From the control panel (CP), power is supplied to the chiller and the centrifugal pump to prepare chilled water up to 10 °C and to circulate it inside the Cu coils of the gas condenser (Gc). The switches are kept ON to operate the

https://doi.org/10.1021/acsomega.3c00908
ACS Omega 2023, 8, 13396−13409

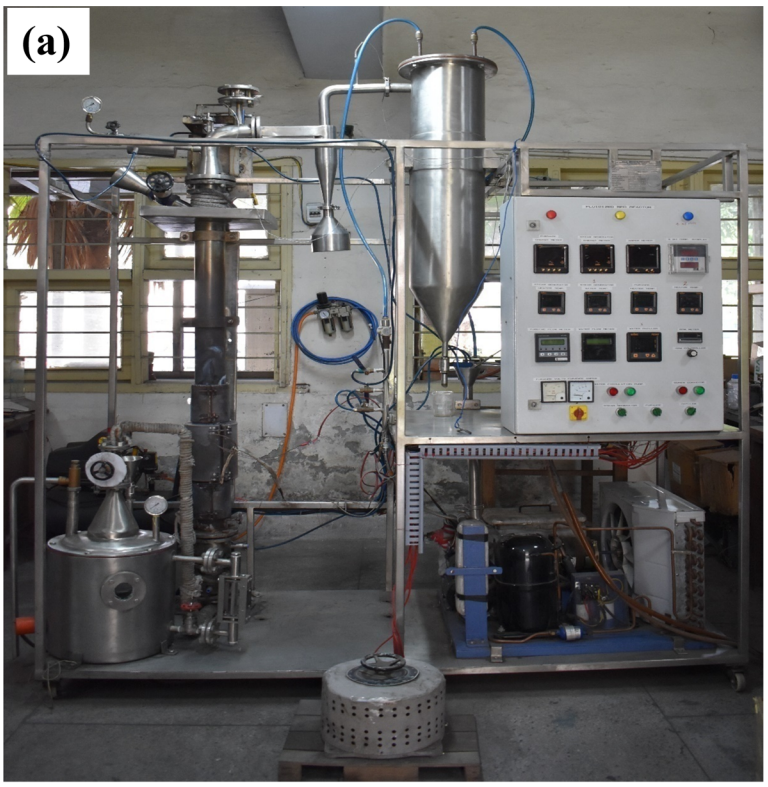

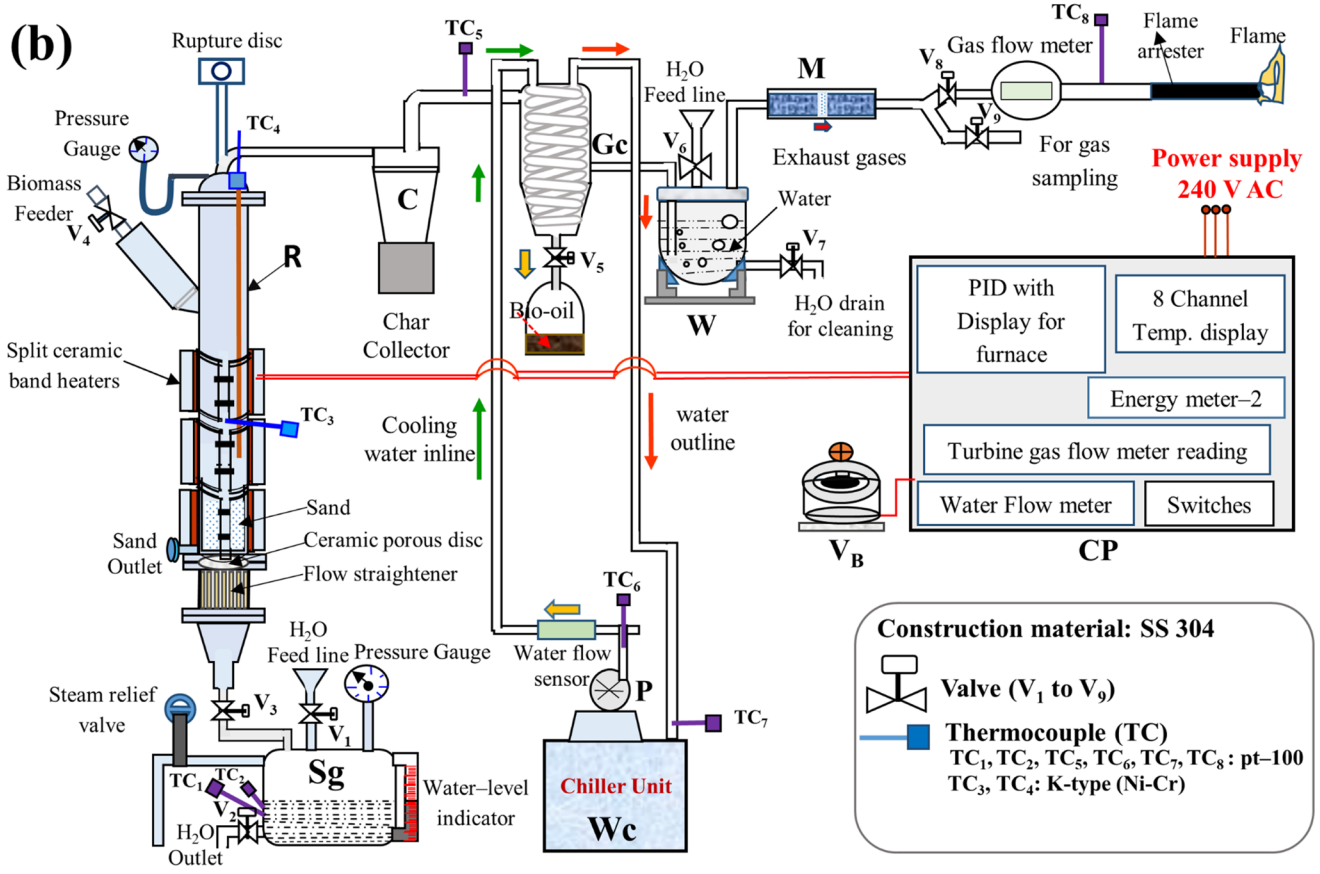

Figure 2. (a) Photograph of the BFB gasifier unit; (b) outline diagram of the BFB gasifier unit.

ceramic band heaters and heaters inside the steam generator. The temperature inside the reactor (R) allows reaching the desired conditions, i.e., 900−1200 K and steaming pressure at 2 kg/cm^2 followed by sufficient preheating conditions (via a nichrome wire). Steam is then passed through the reactor as per a fixed steam-to-biomass ratio ($0 \leq SBR \leq 2$) via valve

https://doi.org/10.1021/acsomega.3c00908
ACS Omega 2023, 8, 13396−13409

Table 1. Description of Individual Units of the Bubbling Fluidized-Bed Gasifier (BFBG)

Sl. no.	unit	specifications	function/purpose(s)
1	steam generator (Sg)	water intake capacity = 15 L; heater capacity = 6 kW; working pressure ≤ 3 kg/cm^2	superheated steam out of Sg is used as the fluidizing gas and is fed into the reactor (R).
2	flow straightener with a porous disk	a bunch of Cu tubes (40 mm length *X* 6 mm diameter) arranged vertically and gas-welded (referred to as the "flow straightener") and a ceramic porous disk of 20−50 μm pore size is placed above the flow straightener.	it is used to maintain the straight and uniform flow of superheated steam at the bottom of the fluidized bed. The ceramic porous disk allows the air−steam to pass through it so that the sand above the disk can be fluidized.
3	reactor (R)	material: stainless steel 304; working temperature ≤ 1200 °C; L X O.D. = 1.5 m × 0.102 m; wall thickness = 3 mm	converts biomass into syngas at high temperatures. The main reactions involved during this conversion with descriptive statements are provided in Table 2.
4	split ceramic band heater with insulation Jacket	the heating element is made of Kanthal-A inner wire; heater capacity = 6 kW (2 kW for each); 230 V is maintained using a voltage barrier (V_B); insulated with a 2−3 cm thick layer of ceramic wool; temperature was controlled by a PID controller	used to heat the reactor up to the desired set point temperature, and an insulator is used to prevent heat loss from the gasifier to the surrounding.
5	cyclone separator (C)	L × I.D. = 40 cm × 8 cm	separates char and dust particles from the syngas coming from the reactor.
6	gas coil condenser (Gc)	L × I.D. = 70 cm × 20 cm; has two helical copper coils (12.5 mm I.D. each) inside Gc.	used for the separation of permanent gases (mainly CO, CO_2, H_2, and CH_4) from the condensable vapors coming from the cyclone separator (C).
7	water tank (W)	L × O.D. = 23 cm × 23 cm	for the separation of tars and reaming dust particles from the gases.
8	moisture trap (M)	silica beads	to remove moisture from the wet gas.
9	turbine gas flow meter with totalizer	Model: TEM-11	to quantify the total volume (in liter) and volumetric flow rate (in liter/h) of gas produced for a particular run.
10	flame arrestor	inline flame arrestor (both sides open)	does not allow the flame of the gas burner to pass against the flow direction of gas.
11.	chiller unit (Wc)	capacity = 10 L of water; flow of cooling water is maintained by a 1/4th HP-centrifugal pump (P).	supply of chilled water (≤10 °C) to the Gc unit, to condense the vapor.
12.	gas burner		used to burn syngas coming out from the flame arrestor.
13.	other auxiliaries		
	thermocouples	pt-100 for ≤300 °C and K-type for ≤1200 °C	to sense the temperature within a calibrated error of 0.02%
	PID controllers	Model: TC203 and TC344	to regulate the temperature
	gaskets	steam and jacketed gaskets	up to 300 °C, leakage is prevented using steam gaskets. The jacketed gaskets (Cu-graphite-SS304) are used to sustain the leak-proof flow of steam and product gases at high temperatures (>650 °C).
	Rupture disk	material: SS 304	to protect from the overpressure within the system, it bursts as the pressure inside the gasifier increases above 2.5 kg/cm^2

https://doi.org/10.1021/acsomega.3c00908
ACS Omega 2023, 8, 13396−13409

Table 2. Rate Constant, Thermodynamics, and Descriptive Statements of Gasification Reactions

reaction	$C + CO_2 \leftrightarrow 2CO$	$C + H_2O \leftrightarrow CO + H_2$	$C + 2H_2 \leftrightarrow CH_4$	$CH_4 + H_2O \leftrightarrow CO + 3H_2$	$CO + H_2O \leftrightarrow CO_2 + H_2$
reaction name	Boudouard reaction	steam gasification	H_2 gasification	methane−steam reforming (MSR)	water−gas shift (WGS)
reaction number	R_1	R_2	R_3	R_4	R_5
nature of reaction	endothermic	endothermic	exothermic	endothermic	exothermic
apparent rate constant (k_{ai}; $k_{ai} = A_i \times \exp\left(-\frac{E_{ai}}{RT}\right)$, unit: s^{-1})	$k_{a1}(T) = 36.16 \times \exp\left(-\frac{77.39}{0.008314 \times T}\right)$	$k_{a2}(T) = 1.517E+04 \times \exp\left(-\frac{121.62}{0.008314 \times T}\right)$	$k_{a3}(T) = 4.189E-03 \times \exp\left(-\frac{19.21}{0.008314 \times T}\right)$	$k_{a4}(T) = 7.301E-02 \times \exp\left(-\frac{36.15}{0.008314 \times T}\right)$	$k_{a5}(T) = 2.824E-02 \times \exp\left(-\frac{32.84}{0.008314 \times T}\right)$
equilibrium rate constant ($k_{pi} = k_{pi}(T)$)	900 K = 0.18	900 K = 0.4	900 K = 0.32	900 K = 1.258	900 K = 2.247
	1000 K = 1.78	1000 K = 2.492	1000 K = 0.0991	1000 K = 25.13	1000 K = 1.4
	1100 K = 11.44	1100 K = 11	1100 K = 0.03737	1100 K = 294.3	1100 K = 0.9612
	1150 K = 24.365	1150 K = 19.807	1150 K = 0.025	1150 K = 824.443	1150 K = 0.739
	1200 K = 51.271	1200 K =35.813	1200 K = 0.017	1200 K = 2203.625	1200 K = 0.635
descriptive statements	as the reaction temperature reaches 973 K ($k_{p1} = 1$ and $\Delta G = 0$), this reaction shifts completely in the forward direction. After that, due to its endothermic nature, the reaction is supposed to be conducted at higher temperatures (here, 1200 K) to obtain the maximum amount of CO gas (Le Chatelier's principle). Therefore, a high temperature is favored for maximum consumption of CO_2 by this reaction.	similar to R_1, as the reaction temperature reaches 950 K ($k_{p2} = 1$ and $\Delta G = 0$), the reaction shifts completely in the forward direction. After that, due to its endothermic nature, this reaction is supposed to be conducted at higher temperatures (here, 1200 K) to obtain the maximum amount of H_2 and CO gas (Le Chatelier's principle).	as the temperature value increases from 900 to 1200 K, higher the shifting of reaction in the backward direction due to its exothermic nature. Thus, gives highest H_2 gas yield at 1200 K.	as the temperature value increases from 900 to 1200 K, higher the tendency to move the reaction in the forward direction. Thus, a reaction of methane with steam at 1200 K gives highest H_2 and CO gas yield.	due to its exothermic nature, this reaction is supposed to conduct at lower temperature (900 K) to get maximum amount of H_2 gas (Le Chatelier's principle). As the temperature reaches at 1090 K ($k_{p5} = 1$ and $\Delta G = 0$), the reaction (R_5) shifts completely in the backward direction. Thus, gives highest amount of H_2 gas at 900 K.

https://doi.org/10.1021/acsomega.3c00908
ACS Omega 2023, 8, 13396−13409

"V_3" to fluidize the sand inside the reactor and also provide a gasifying medium for biomass gasification. For steam at 900 K, the minimum fluidization velocity of sand particles (U_{mf}) is maintained at 0.104 m/s, and to achieve this, the velocity of steam at the exit of the steam generator is fixed at 0.21 m/s. Eucalyptus wood sawdust (EWS) is fed into the reactor (R) through a biomass feeder, and after injecting the feed mixture into the reactor, the valve "V_4" is immediately closed.

The reaction temperature is measured by a *K*-type thermocouple (Ni−Cr), placed at the center of R, touching the sand. As the experiment reached the desired conditions of operating parameters, biomass was fed into the reactor (R), and the gas sample was collected in a Tedlar bag. The leftover gases are burnt at the exit of the flame arrester. During the whole process, steam is regularly injected with a specific flow rate to continue the fluidization during the gasification process. At the end of the process, after cooling down the setup, the solid remaining (char) inside the reactor was screened from the sand; bio-oil from the bottom of Gc and dust from the dust collector were collected, and their weights were measured to calculate the conversion efficiency.

2.4.3. Collection and Storage of the Final Product. The feed mixture gasifies in the reactor as it is exposed to high temperatures (here, 900−1200 K). The main reactions involved in the air−steam gasification of eucalyptus wood sawdust are provided in Table 2. At an elevated temperature, this sawdust is converted into a gaseous mixture (mainly H_2, CO, CH_4, and CO_2). The gases produced in the reactor (R) move toward the cyclone separator where char and tiny silica sand particles (accompanied by gases due to the fluidization) are separated from the gases and are collected in the char collector. The clean gases that come out from the exit of the cyclone separator move toward the gas condenser (Gc), where these gases are sufficiently cooled down to 10 °C so that the noncondensable gases present in it can be separated. The noncondensable gases are then passed through a water tank (W), where the tar and remaining dust particle are settled down. The gases coming from the water tank (W) are passed through a moisture trap (M) to trap all of the moisture present in it. Further, to measure the volumetric flow rate along with the total amount of product gas formed, the moisture-free syngas is passed through a turbine gas flow meter with a totalizer (model: TEM-11). The exit gases from the flow meter are collected in a Tedlar bag for gas sampling in GC (NEWCHROME 6700), and the remaining gases are burned using a gas burner after passing these through an inline flame arrestor (model: 872). At the end of each experimental run, steam is used to flush out all of the existing gases within the experimental unit.

2.5. Calculation of the Performance Parameters. The chemical kinetic model of the EWS yields various syngas compositions for different sets of operating parameters. However, the feasibility of the gasifier and the usability of the biomass cannot be measured by calculating only the vol % of the syngas composition. Therefore, separate performance parameters need to be calculated in order to measure the performance of the EWS biomass gasification process. The model performance is evaluated in terms of the H_2 gas and syngas yields (g/kg of biomass feed), lower heating value (LHV), higher heating value (HHV), cold gas efficiency (CGE), carbon conversion efficiency (X_C), and gasification efficiency (GE). The expressions for the above performance parameters are given below

The H_2-gas yield (HGY) and syngas yield (SGY) are defined as follows[38]

$$\mathrm{HGY} = \left(\frac{\text{total mass of } H_2\text{(g) in syngas}}{\text{total biomass feeded}}\right) = \left(\frac{x_2 \times \text{mol. wt. of } H_2}{\text{mol. wt. of EWS biomass}}\right) \quad (25)$$

and

$$\mathrm{SGY} = \left(\frac{\text{total mass of syngas}}{\text{total biomass feeded}}\right) = \left(\frac{x_2 \times \text{mol. wt. of } H_2 + x_3 \times \text{mol. wt. of CO}}{\text{mol. wt. of EWS biomass}}\right) \quad (26)$$

where, x_2 and x_3 are the moles of H_2 and CO gas, respectively.

The LHV and HHV of the produced gases are defined as follows[39]

$$\mathrm{LHV_{gas}(in\ MJ/Nm^3)} = (25.76 \times C_{H_2} + 30.18 \times C_{CO} + 85.78 \times C_{CH_4}) \times 0.0042 \quad (27)$$

$$\mathrm{HHV_{gas}(in\ MJ/Nm^3)} = (30.52 \times C_{H_2} + 30.18 \times C_{CO} + 95 \times C_{CH_4}) \times 0.0041868 \quad (28)$$

Based on the LHV of syngas and biomass feed, the cold gas efficiency (CGE) is defined as follows[5]

$$\mathrm{CGE} = \left(\frac{\mathrm{LHV_{gas}}}{\mathrm{LHV_{biomass}} + \text{energy content of steam}}\right) \quad (29)$$

The carbon conversion efficiency is defined as follows[40]

$$X_C = \left(\frac{\text{total moles of carbon reacted in the biomass sample}}{\text{total moles of carbon in fresh biomass}}\right) \quad (30)$$

On the other hand, the gasification efficiency is based on the total moles of syngas produced. The gasification efficiency (GE) is defined as follows[5]

$$\mathrm{GE} = \left(\frac{\text{total mass of syngas}}{\text{total biomass feed}}\right) \quad (31)$$

3. RESULTS AND DISCUSSION

3.1. EWS Biomass Characterization. Table 3 presents all the necessary characterizations of the EWS sample representing its moisture and ash content (<10 wt %), indicating its favorability as an alternate fuel.[41,42] The required amount of volatiles in EWS (75.38 wt %) assist in the thermal conversion process, resulting in more combustible gases during the conversion, which leads to H_2-rich syngas production at high temperatures (>700 °C). Higher amounts of fixed carbon (14.70 wt %) and hydrogen (5.462 wt %) indicate its usability as a better biomass material for H_2 gas production. No traces of S and N are found in the sample, which implies no risk of greenhouse gas emission during its ignition. Using the CHNS/O data, the empirical formula of the EWS biomass is calculated

https://doi.org/10.1021/acsomega.3c00908
ACS Omega 2023, 8, 13396−13409

Table 3. Characterization of the As-Received Sample of EWS

	EWS
proximate analysis (wt %)	
moisture	7.76
volatile content	75.38
ash	2.16
fixed carbon[a]	14.70
elemental analysis (wt %)	
carbon (C)	40.12
hydrogen (H)	5.462
nitrogen (N)	N/A
sulfur (S)	N/A
oxygen (O[b])	54.418
H/C atomic ratio (α)	1.63
O/C atomic ratio (β)	1.02
empirical formula	$CH_{1.63}O_{1.02}$
heating values (MJ/kg)	
LHV	13.48
HHV	14.77

[a]Fixed carbon = 100 − (moisture + volatile content + ash). [b]Oxygen content = 100 − (C + H + N + S).

as $CH_{1.63}O_{1.02}$ (where α = 1.63 and β = 1.02).[43] The lower and higher heating values, i.e., LHV and HHV, of the EWS biomass are computed to be 13.48 and 14.77 MJ/kg, respectively.

3.2. Validation of the Model. The present study utilized chemical kinetic modeling with a water−gas shift reaction where an in-house built FORTRAN code has been developed in order to solve the reaction equations. Before conducting any case study, it is important to check whether the simulation results are acceptable or not and whether validation is required. Hence, simulation results are compared with available experimental results for a given set of conditions. For the first case, i.e., pine sawdust as biomass material at T = 950 °C, ER = 0.2, SBR=1.02, calcined cement = 0 wt %, the present kinetic model accurately predicts the gas composition obtained by experimental results,[16] and the RMSE value is found to be 2.56. Similarly, when almond shells are used as the feedstock material at T = 770 °C, fluidized bed of silica sand, and SBR = 1, the kinetic model closely predicts the gas composition obtained by experimental analysis,[44] where the RMSE was found to be 3.04. However, when considering cornstalk[45] as the feedstock material, the gas composition, mainly H_2, obtained by the kinetic model, slightly deviates from the experimental result although the overall RMSE value is calculated to be 3.67, the maximum value compared to other cases. These three different types of biomass materials and RMSE values indicate that the present kinetic model fits well for woody biomass. In addition, some experiments are performed on the lab scale, and the results are compared with those of the present kinetic model, which shows the maximum RMSE of 3.38. Table 4 shows a comparison of the results obtained by the present kinetic model and the experimental work, and the mean value of the RMSE obtained is 3.09, which is well within the acceptable range.

This validation gives the confidence to perform further analysis, using the FORTRAN code, for different case studies.

3.3. Effect of Reaction Temperature. One of the crucial operating parameters that influence the production of syngas inside the bubbling fluidized-bed gasifier (BFBG) is the gasifier temperature. Figure 3 demonstrates the effect of gasification

Table 4. Comparison of the Present Model Data of Syngas Composition (vol %) with the Experimental Results

			experimental values[16]				model predicted				
biomasses	system type	operating parameters	H_2	CO	CO_2	CH_4	H_2	CO	CO_2	CH_4	RMSE[a]
Pine sawdust	air−steam gasification in a fluidized-bed gasifier	T = 950 °C, ER = 0.2, SBR=1.02, calcined cement = 0 wt %	37.73	36.56	19.94	4.31	37.48	37.45	23.89	1.18	2.56
			experimental values[44]				model predicted				
Almond shells	steam gasification in a fluidized-bed gasifier	T = 770 °C, fluidized bed of silica sand, SBR = 1	43.6	33.2	11.7	11.5	38.95	36.45	13.77	10.83	3.04
			experimental values[45]				model predicted				
Cornstalk	steam gasification in a fluidized-bed gasifier	T = 700 °C, sorbent-to-biomass ratio = 0, SBR = 1	36.2	36.42	17.38	10	42.39	33.33	16.56	7.72	3.67
			experiments (present study)				model predicted				
Eucalyptus wood sawdust	bubbling fluidized-bed gasifier	P = 1 atm, ER = 0, SBR = 0.75, Dp = 100 μm, T = 1000 K	48.02	34.06	11.33	6.59	47.47	32.74	16.27	3.52	2.99
		P = 1 atm, ER = 0, SBR = 2, Dp = 100 μm, T = 1100 K	52.04	31.82	11.61	4.53	49.22	30.78	17.21	2.79	3.29
		P = 1 atm, ER = 0, SBR = 0.75, Dp = 1000 μm, T = 1100 K	53.16	32.04	10.33	4.47	51.98	31.61	15.76	0.65	3.38
		P = 1 atm, ER = 0.1, SBR = 0.75, Dp = 100 μm, T = 1000 K	43.65	34.43	16.44	5.48	42.88	31.76	20.94	4.42	2.70

[a]$\mathrm{RMSE} = \sqrt{\frac{\sum_{i=1}^{n}(y_{\exp,i} - y_{\mathrm{sim},i})^2}{n}}$.

https://doi.org/10.1021/acsomega.3c00908
ACS Omega 2023, 8, 13396−13409

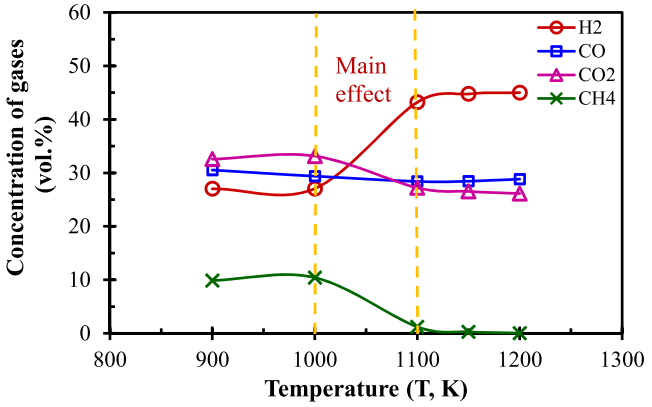

Figure 3. Effect of temperature on the gaseous product composition (ER = 0.25, SBR = 1, Dp = 100 μm, P = 1 atm).

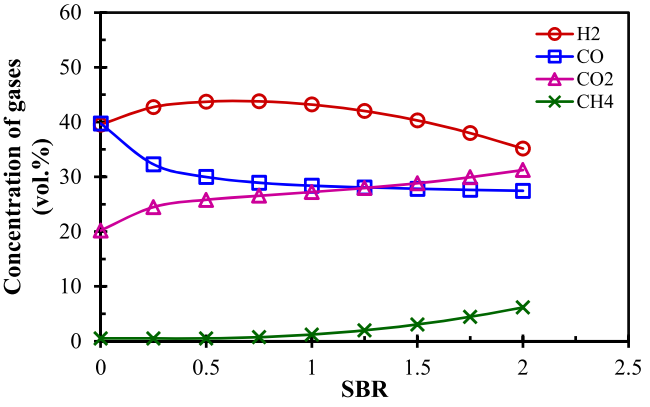

Figure 4. Effect of the steam-to-biomass ratio on the gaseous product composition (T = 1100 K, ER = 0.25, Dp = 100 μm, P = 1 atm).

temperature (900−1200 K) on the product gas composition. The graph shows that increasing temperature results in an increase in the volumetric percentage of H_2-rich syngas. Gasification products (vol %) are the results of the combined effect of reactions R_1−R_5. On increasing the temperature from 900 to 1000 K, reactions R_2, R_3, and R_4 promote higher hydrogen production, whereas reactions R_1 and R_5 retard hydrogen production. This can also be confirmed on the basis of the combined spontaneity and nonspontaneity of gasification reactions. On increasing the temperature from 900 to 1000 K, the level of spontaneity increases for R_1, R_2, and R_4 reactions, whereas it decreases for R_5, and R_3 becomes highly nonspontaneous. In the temperature range of 900−1000 K, the concentration of gaseous products shows negligible change, and this can be verified by the change in the equilibrium rate constant of gaseous reactions (R_1−R_5), as shown in Table 2. As the temperature is increased from 1000 to 1100 K, CO_2 and CH_4 gases show a decreasing trend, whereas H_2 shows an increasing trend. This trend of CO_2 and CH_4 occurs because there is a decrease in the equilibrium values of R_3 and R_5, whereas for H_2, there is a rapid increase in the k_p values of R_1, R_2, and R_4 reactions. Carbon monoxide (CO) initially remained almost constant from 900 to 1000 K and then decreased from 29.38 to 28.83 vol %. The CO content that was originally formed by the primary and secondary devolatilization reactions showed an initial slow decreasing trend as it reacted with H_2O in the WGS reaction (R_5), creating H_2.

It can be observed that changes in gas concentration are not significant beyond 1100 K. For H_2, after 1100 K, an increment of the temperature of 100 K (i.e., at 1200 K) resulted in an increase in only 1.80 vol %. Therefore, this small increase in H_2 gas production cannot be compensated by a large amount of input energy, i.e., 100 K increase. Hence, 1100 K can be opted as the optimum reaction temperature for maximizing H_2-rich syngas production. Similar effects were also observed by Cao et al.[28] for pine sawdust.

3.4. Effect of Steam-to-Biomass (SBR) Ratio. In the gasification process, steam is commonly preferred over other gasifying media as steam highly stimulates the calorific value of the product gas by adding to the volumetric concentration of H_2 gas. Hence, the steam-to-biomass ratio is a significant parameter affecting the quality of syngas production mainly for H_2 gas. Figure 4 depicts the variation in gas composition with the steam-to-biomass ratio (SBR). As can be seen, with an increase in SBR from 0 to 0.75, H_2 increased from 39.53 to 43.79 vol %, as the WGS reaction (R_5) is promoted at a higher SBR. An increase in the steam-to-biomass ratio increases the moles of H_2O(g), as shown in eq 1, and therefore accelerates the water−gas shift (WGS) reaction. This results in the enrichment of the H_2 and CO_2 production and makes the water−gas shift reaction a vital one in EWS biomass gasification. It is to be noted that the Wang and Kinoshita kinetic model[21] neglected the WGS reaction, although the present model considers that this model yields results closer to the actual chemical reaction occurring in the gasifier. The steam addition benefited methane production due to the enhancement of the methane−steam reforming reaction (rev-R_4). On further increasing the SBR value above 0.75, the additional steam increases both the biomass gasification cost and the CO_2 component, which leads to a reduction in the H_2 content. In this study, as the SBR increases from 0.75 to 2, the H_2 content in the outlet gases reduces from 43.79 to 35.16 vol % and CO_2 increases from 26.56 to 31.25 vol %, and thus, 0.75 is considered as the optimal value of SBR.

3.5. Effect of Particle Size. Chemical reaction rates are influenced by the particle size through the overall surface area of biomass. Figure 5 illustrates the effect of biomass (char) particle diameter on product gas compositions at steady-state conditions. It can be seen that with an increase in particle size from 100 to 1000 μm, the composition of product gases (vol %) is negligibly affected. This is because, with a smaller char particle diameter, the surface area exposed to the heating zone is greater compared to that of coarse particles. In addition, a

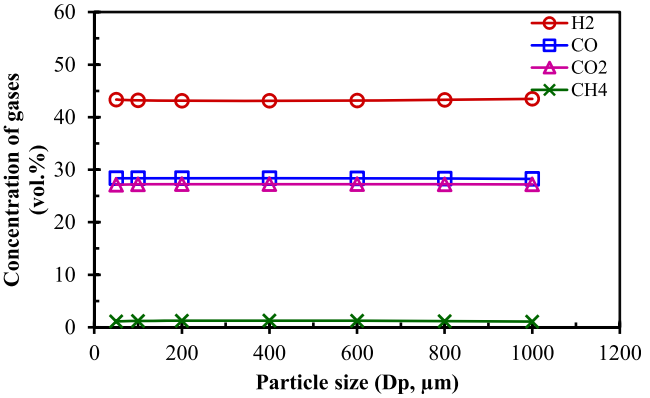

Figure 5. Effect of particle size on the gaseous product composition (T = 1100 K, ER = 0.25, SBR = 1, P = 1 atm).

https://doi.org/10.1021/acsomega.3c00908
ACS Omega 2023, 8, 13396−13409

small char particle size supports the fluidization process in the gasifier. Hence, finer char particles initially yield higher concentrations of product gases, whereas coarse particles yield lower concentrations. However, as the simulation is completed at steady-state conditions, both finer and coarse particles have minor effects on the product gas compositions, no matter how fast or slow the gases are produced. For a fixed amount of biomass, an increased particle size corresponds to decreased biomass surface area, which reduces the surface reaction rate; thus, a longer residence time is needed to achieve the same conversion ratio.

3.6. Effect of Equivalence Ratio (ER). Computational results for varying equivalence ratios are presented in Figure 6.

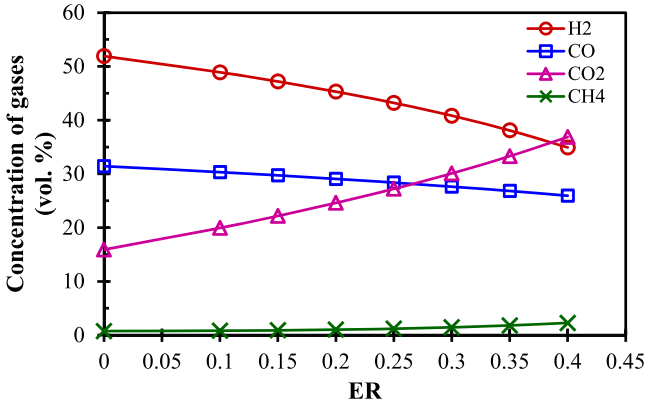

Figure 6. Effect of the equivalence ratio on the gaseous product composition (T = 1100 K, SBR = 1, Dp = 100 μm, P = 1 atm).

By increasing the ER from 0 to 0.4, the CO_2 (15.91−36.85 vol %) and CH_4 (0.74−2.28%) contents increase, while H_2 (51.91−34.92%) and CO (31.44−25.95%) contents decrease. Out of these, H_2 and CO_2 are highly affected, as the ER increases due to increased oxygen in the reactants. The highest volumetric concentration of H_2 gas (51.91%) was obtained at ER = 0.

The equivalence ratio is one of the most important parameters in biomass gasification, and determining the optimal ER value plays a major role in the energy, economic, and environmental aspects of biomass gasification. As the ER increased from 0 to 0.4, H_2 decreased from 51.91 to 34.92 vol %. An increase in the ER value indicates an enriching oxidizer (air), leading to a shift of the gasification reaction toward the combustion region, which means a reduction in energetic compounds and an increase in greenhouse gas emission. An increase in CH_4 content from 0.75 to 2.28 vol % at higher ER is caused by the reverse methane−steam reforming reaction (rev-R_4), which is promoted by the enriched oxidant. As a result of this reaction, the ER increases from 0 to 0.4 and the CO concentration decreases from 31.43 to 25.95 vol %.

3.7. Effect of Pressure. Normally, gasification experiments are performed in lower pressure conditions, usually 1 atm, and in order to investigate the feasibility of higher pressures on H_2 gas production, simulations are performed. Computational results of varying pressures are depicted in Figure 7. An increase in pressure from 1 to 20 atm results in higher yields of CO_2 and CH_4 and lower yields of H_2 and CO, and this is due to a shift in the equilibrium. Pressure in the gasifier regulates the residence time of the gaseous species and thus influences the product gas composition. The composition could be altered via interactive reactions among gaseous species. At low

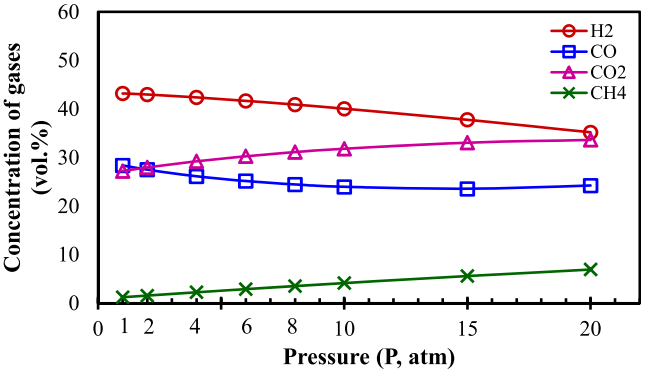

Figure 7. Effect of pressure on gaseous product composition (T = 1100 K, ER = 0.25, SBR = 1, and Dp = 100 μm).

pressure, a higher exposure time of gaseous species leads to higher H_2-rich syngas production. At high pressure, a lower exposure time of gaseous species in the gasifier (at T = 1100 K) leads to high CO_2 and low H_2-rich syngas production. As per Le Chatelier's principle, gasification reactions are generally favored at lower pressure.[46] The overall result indicates that higher pressure suppresses H_2-rich syngas production and thus is no longer beneficial to the gasification process. Hence, a lower pressure is usually preferred because of the cost of the material construction and safety concerns. The results of this study are consistent with the earlier observation by Hantoko et al.[46]

3.8. Optimizing H_2 Content. Generally, the aim of biomass gasification is to improve syngas production with the maximum contribution from hydrogen gas because of its higher calorific value. In the present study, there are five parameters considered to understand its effect on the gas composition, as shown in Figures 3−7. From the above analysis, one can observe that the aforesaid parameters have either a positive or a negative effect on H_2-rich syngas production, and hence the optimum setting must be found, which yields the maximum value of the H_2 component. It is concluded that parameters of P = 1 atm, ER = 0, SBR = 0.75, Dp = 100 μm, and T = 1100 K provide the optimum setting, wherein the production of H_2 gas is the maximum. Using this parametric setting, the present chemical kinetic model yields 51.81 vol % H_2 gas composition. In order to verify the simulation results, three experiments are performed with the same setting, where the experimental result (55.04 ± 0.81 vol % of H_2) is closer to that of the kinetic model. Figure 8 depicts a comparison of the results, for maximum H_2 production, obtained by the kinetic model and the experiment. The performance parameters, calculated for both the experiment and the kinetic model, are shown in Table 5.

4. CONCLUSIONS

The kinetic model for the gasification of eucalyptus wood sawdust is developed based on the surface kinetics using the Langmuir−Hinshelwood mechanism. The developed model is validated with the experimental literature data as well as data obtained by lab-scale experiments performed on a bubbling fluidized-bed gasifier. The chemical kinetic model data are found to be in good agreement with the experimental data. Simulations are performed to address the effects of five operating parameters, including temperature, equivalence ratio, steam-to-biomass ratio, pressure, and particle size, on product

https://doi.org/10.1021/acsomega.3c00908
ACS Omega 2023, 8, 13396−13409

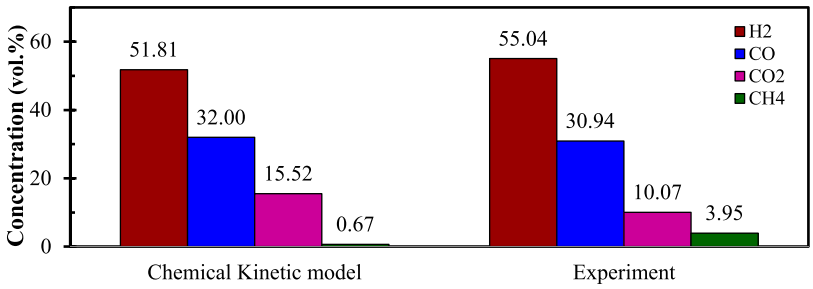

Figure 8. Validation run at the optimum conditions of operating parameters (P = 1 atm, ER = 0, SBR = 0.75, Dp = 100 μm, T = 1100 K).

Table 5. Evaluation of the Performance Parameters for the Maximum H_2 Gas Production

	(ER=0,SBR=0.75,P=1atm,Dp=100μm,T=-1100 K)	
output	experimental	kinetic model
H_2 (vol %)	55.04	51.81
HGY (g H_2/g EWS)	0.076	0.072
SGY (g syngas/g EWS)	0.677	0.693
LHV (MJ/Nm^3)	11.30	9.90
HHV (MJ/Nm^3)	12.51	10.93
CGE (%)	71.99	63.10
X_C	27.90	29.91
GE (%)	67.75	69.35

gas compositions. Results show that the maximum values of 59.84 and 10.76% improvements of H_2 are seen with increases in the temperature and steam-to-biomass ratio, respectively, whereas 32.73 and 18.54% decreases are noticed with increases in the equivalence ratio and pressure, respectively. It is worth mentioning that there is hardly any effect of the char particle size on the production of any of the gas contents. In order to achieve the maximum utilization of biomass gasification, an optimum set of operating parameters is found that gives the maximum value of the H_2 gas component. Parameters such as P = 1 atm, ER = 0, SBR = 0.75, Dp = 100 μm, and T = 1100 K are found to be optimum, and results obtained by the kinetic model are validated with experimental results. From the performance parameters, higher HGY and CGE, i.e., 0.072 g-H_2/g-EWS and 63.10% (kinetic model) [0.076 g-H_2/g-EWS and 71.99% using the experimental method], indicate the potential of eucalyptus wood sawdust as the gasification feedstock. In the near future, the developed chemical kinetic model can be further modified by incorporating a sorbent reaction in the gasification process.

AUTHOR INFORMATION

Corresponding Author

Ajay Sharma − *Department of Chemical Engineering, Indian Institute of Technology Roorkee, Roorkee 247667 Uttarakhand, India;* orcid.org/0000-0002-7092-1249; Email: asharma@ch.iitr.ac.in

Author

Ratnadeep Nath − *Department of Mechanical Engineering, National Institute of Technology Mizoram, Aizawl 796012, India*

Complete contact information is available at: https://pubs.acs.org/10.1021/acsomega.3c00908

Notes

The authors declare no competing financial interest.

ACKNOWLEDGMENTS

This research work is dedicated to our beloved professor B. Mohanty (Late), IIT Roorkee. His continuous effort, inspiration, and guidance motivated the authors to produce quality work. Professor Mohanty's conceptualization helped frame this research article.

NOMENCLATURE

A_i	Preexponential factor of the ith reaction (s$^-$))
ASTM	American Society for Testing and Materials
BFBG	bubbling fluidized-bed gasifier
CGE	cold gas efficiency
EWS	Eucalyptus wood sawdust
ER	equivalence ratio
E_{ai}	apparent activation energy of the ith reaction (kJ/mol)
GE	gasification efficiency
HGY	hydrogen gas yield
HHV	higher heating value
K_i	adsorption constant for the ith gas species
k_{ai}	apparent rate constant for the ith reaction (s^{-1})
k_{pi}	equilibrium constant for the ith reaction
LHV	lower heating value
MSR	methane−steam reforming
R	universal gas constant (kJ/mol K)
RMSE	root-mean-square error
SGY	syngas yield
SBR	steam-to-biomass ratio
w	moles of water
WGS	water−gas shift
x	moles of product species
X_C	carbon conversion efficiency (%)
y	moles of oxygen
z	moles of nitrogen

Greek letters

μ	steam-to-carbon dioxide ratio
α	hydrogen-to-carbon atomic ratio
β	oxygen-to-carbon atomic ratio

REFERENCES

(1) Ahmadi, P.; Khoshnevisan, A. Dynamic Simulation and Lifecycle Assessment of Hydrogen Fuel Cell Electric Vehicles Considering Various Hydrogen Production Methods. *Int. J. Hydrogen Energy* **2022**, *47*, 26758−26769.

(2) Holmlid, L.; Kotarba, A.; Stelmachowski, P. Production of Ultra-Dense Hydrogen H(0): A Novel Nuclear Fuel. *Int. J. Hydrogen Energy* **2021**, *46*, 18466−18480.

(3) Okolie, J. A.; Mukherjee, A.; Nanda, S.; Dalai, A. K.; Kozinski, J. A. Catalytic Supercritical Water Gasification of Soybean Straw: Effects

https://doi.org/10.1021/acsomega.3c00908
ACS Omega 2023, 8, 13396−13409

of Catalyst Supports and Promoters. *Ind. Eng. Chem. Res.* **2021**, *60*, 5770−5782.
(4) Mohamadi-Baghmolaei, M.; Zahedizadeh, P.; Hajizadeh, A.; Zendehboudi, S. Hydrogen Production through Catalytic Supercritical Water Gasification: Energy and Char Formation Assessment. *Energy Convers. Manage.* **2022**, *268*, No. 115922.
(5) Shahbaz, M.; Yusup, S.; Inayat, A.; Ammar, M.; Patrick, D. O.; Pratama, A.; Naqvi, S. R. Syngas Production from Steam Gasification of Palm Kernel Shell with Subsequent CO2 Capture Using CaO Sorbent: An Aspen Plus Modeling. *Energy Fuels* **2017**, *31*, 12350−12357.
(6) Salaudeen, S. A.; Acharya, B.; Heidari, M.; Al-Salem, S. M.; Dutta, A. Hydrogen-Rich Gas Stream from Steam Gasification of Biomass: Eggshell as a CO2 Sorbent. *Energy Fuels* **2020**, *34*, 4828−4836.
(7) Han, L.; Wang, Q.; Yang, Y.; Yu, C.; Fang, M.; Luo, Z. Hydrogen Production via CaO Sorption Enhanced Anaerobic Gasification of Sawdust in a Bubbling Fluidized Bed. *Int. J. Hydrogen Energy* **2011**, *36*, 4820−4829.
(8) Tursun, Y.; Xu, S.; Wang, C.; Xiao, Y.; Wang, G. Steam Co-Gasification of Biomass and Coal in Decoupled Reactors. *Fuel Process. Technol.* **2016**, *141*, 61−67.
(9) Maisano, S.; Urbani, F.; Cipitì, F.; Freni, F.; Chiodo, V. Syngas Production by BFB Gasification: Experimental Comparison of Different Biomasses. *Int. J. Hydrogen Energy* **2019**, *44*, 4414−4422.
(10) Soria, J.; Li, R.; Flamant, G.; Mazza, G. D. Influence of Pellet Size on Product Yields and Syngas Composition during Solar-Driven High Temperature Fast Pyrolysis of Biomass. *J. Anal. Appl. Pyrolysis* **2019**, *140*, 299−311.
(11) Alauddin, Z. A. B. Z.; Lahijani, P.; Mohammadi, M.; Mohamed, A. R. Gasification of Lignocellulosic Biomass in Fluidized Beds for Renewable Energy Development: A Review. *Renewable Sustainable Energy Rev.* **2010**, *14*, 2852−2862.
(12) Rodriguez, R.; Mazza, G.; Fernandez, A.; Saffe, A.; Echegaray, M. Prediction of the Lignocellulosic Winery Wastes Behavior during Gasification Process in Fluidized Bed: Experimental and Theoretical Study. *J. Environ. Chem. Eng.* **2018**, *6*, 5570−5579.
(13) Ahmad, A. A.; Zawawi, N. A.; Kasim, F. H.; Inayat, A.; Khasri, A. Assessing the Gasification Performance of Biomass: A Review on Biomass Gasification Process Conditions, Optimization and Economic Evaluation. *Renewable Sustainable Energy Rev.* **2016**, *53*, 1333−1347.
(14) Ruiz, J. A.; Juárez, M. C.; Morales, M. P.; Muñoz, P.; Mendívil, M. A. Biomass Gasification for Electricity Generation: Review of Current Technology Barriers. *Renewable Sustainable Energy Rev.* **2013**, *18*, 174−183.
(15) Kumar, A.; Eskridge, K.; Jones, D. D.; Hanna, M. A. Steam-Air Fluidized Bed Gasification of Distillers Grains: Effects of Steam to Biomass Ratio, Equivalence Ratio and Gasification Temperature. *Bioresour. Technol.* **2009**, *100*, 2062−2068.
(16) Sui, M.; Li, G.-y.; Guan, Y.-l.; Li, C.-m.; Zhou, R.-q.; Zarnegar, A. M. Hydrogen and Syngas Production from Steam Gasification of Biomass Using Cement as Catalyst. *Biomass Convers. Biorefin.* **2020**, *10*, 119−124.
(17) Kumari, P.; Mohanty, B. Hydrogen-Rich Gas Production with CO2 Capture from Steam Gasification of Pine Needle Using Calcium Oxide: Experimental and Modeling Study. *Int. J. Energy Res.* **2020**, *44*, 6927−6938.
(18) Vikram, S.; Rosha, P.; Kumar, S.; Mahajani, S. Thermodynamic Analysis and Parametric Optimization of Steam-CO2 Based Biomass Gasification System Using Aspen PLUS. *Energy* **2022**, *241*, No. 122854.
(19) Ratnadhariya, J. K.; Channiwala, S. A. Three Zone Equilibrium and Kinetic Free Modeling of Biomass Gasifier - a Novel Approach. *Renewable Energy* **2009**, *34*, 1050−1058.
(20) Eri, Q.; Peng, J.; Zhao, X. CFD Simulation of Biomass Steam Gasification in a Fluidized Bed Based on a Multi-Composition Multi-Step Kinetic Model. *Appl. Therm. Eng.* **2018**, *129*, 1358−1368.
(21) Wang, Y.; Kinoshita, C. M. Kinetic Model of Biomass Gasification. *Sol. Energy* **1993**, *51*, 19−25.
(22) Echegaray, M.; García, D. Z.; Mazza, G.; Rodriguez, R. Air-Steam Gasification of Five Regional Lignocellulosic Wastes: Exergetic Evaluation. *Sustainable Energy Technol. Assess.* **2019**, *31*, 115−123.
(23) Puig-Gamero, M.; Pio, D. T.; Tarelho, L. A. C.; Sánchez, P.; Sanchez-Silva, L. Simulation of Biomass Gasification in Bubbling Fluidized Bed Reactor Using Aspen Plus. *Energy Convers. Manage.* **2021**, *235*, No. 113981.
(24) Torres-Sciancalepore, R.; Asensio, D.; Nassini, D.; Fernandez, A.; Rodriguez, R.; Fouga, G.; Mazza, G. Assessment of the Behavior of Rosa Rubiginosa Seed Waste during Slow Pyrolysis Process towards Complete Recovery: Kinetic Modeling and Product Analysis. *Energy Convers. Manag.* **2022**, *272*, No. 116340.
(25) Fernandez, A.; Soria, J.; Rodriguez, R.; Baeyens, J.; Mazza, G. Macro-TGA Steam-Assisted Gasification of Lignocellulosic Wastes. *J. Environ. Manage.* **2019**, *233*, 626−635.
(26) Song, Y.; Tian, Y.; Zhou, X.; Liang, S.; Li, X.; Yang, Y.; Yuan, L. Simulation of Air-Steam Gasification of Pine Sawdust in an Updraft Gasification System for Production of Hydrogen-Rich Producer Gas. *Energy* **2021**, *226*, No. 120380.
(27) Champion, W. M.; Cooper, C. D.; Mackie, K. R.; Cairney, P. Development of a Chemical Kinetic Model for a Biosolids Fluidized-Bed Gasifier and the Effects of Operating Parameters on Syngas Quality. *J. Air Waste Manage. Assoc.* **2014**, *64*, 160−174.
(28) Cao, Y.; Bai, Y.; Du, J. Air-Steam Gasification of Biomass Based on a Multi-Composition Multi-Step Kinetic Model: A Clean Strategy for Hydrogen-Enriched Syngas Production. *Sci. Total Environ.* **2021**, *753*, No. 141690.
(29) Fernandez, A.; Sette, P.; Echegaray, M.; Soria, J.; Salvatori, D.; Mazza, G.; Rodriguez, R. Clean recovery of phenolic compounds, pyro-gasification thermokinetics, and bioenergy potential of spent agro-industrial bio-wastes. *Biomass Convers. Biorefin.* **2021**, *0*, 1−18.
(30) Brems, A.; Baeyens, J.; Beerlandt, J.; Dewil, R. Resources, Conservation and Recycling Thermogravimetric Pyrolysis of Waste Polyethylene-Terephthalate and Polystyrene: A Critical Assessment of Kinetics Modelling. *Resour., Conserv. Recycl.* **2011**, *55*, 772−781.
(31) Venier, C. M.; Urrutia, A. R.; Capossio, J. P.; Baeyens, J. Comparing ANSYS Fluent and OpenFOAM Simulations of Geldart A, B and D Bubbling Fl Uidized Bed Hydrodynamics. *Int. J. Numer. Methods Heat Fluid Flow* **2019**, *30*, 93−118.
(32) Sharma, A.; Mohanty, B. Thermal Degradation of Mango (Mangifera Indica) Wood Sawdust in a Nitrogen Environment: Characterization, Kinetics, Reaction Mechanism, and Thermodynamic Analysis. *RSC Adv.* **2021**, *11*, 13396−13408.
(33) Channiwala, S. A.; Parikh, P. P. A Unified Correlation for Estimating HHV of Solid, Liquid and Gaseous Fuels. *Fuel* **2002**, *81*, 1051−1063.
(34) Sharma, A.; Mohanty, B. Non-Isothermal TG/DTG-FTIR Kinetic Study for Devolatilization of Dalbergia Sissoo Wood under Nitrogen Atmosphere. *J. Therm. Anal. Calorim.* **2021**, *146*, 865−879.
(35) Baxter, R. J.; Hu, P. Insight into Why the Langmuir-Hinshelwood Mechanism Is Generally Preferred. *J. Chem. Phys.* **2002**, *116*, 4379−4381.
(36) Wonoputri, V.; Effendy, M.; Wibisono Budhi, Y.; Bindar, Y.; Subagjo. Determination of Kinetic Parameters for Methane Oxidation over Pt/γ-Al2O3 in a Fixed-Bed Reactor. *J. Eng. Technol. Sci.* **2013**, *45 B*, 193−206.
(37) C, S. A Survey of Biomass Gasification Solar Energy Research Institute: US, 1979; Vol. *3*.
(38) Khan, Z.; Yusup, S.; Ahmad, M. M.; Chin, B. L. F. Hydrogen Production from Palm Kernel Shell via Integrated Catalytic Adsorption (ICA) Steam Gasification. *Energy Convers. Manage.* **2014**, *87*, 1224−1230.
(39) Zha, Z.; Wang, K.; Ge, Z.; Zhou, J.; Zhang, H. Morphological and Heat Transfer Characteristics of Biomass Briquette during Steam Gasification Process. *Bioresour. Technol.* **2022**, *356*, No. 127334.

https://doi.org/10.1021/acsomega.3c00908
ACS Omega 2023, 8, 13396−13409

(40) Ahmad, N. A.; Al-attab, K. A.; Zainal, Z. A.; Lahijani, P. Microwave Assisted Steam - CO2 Char Gasification of Oil Palm Shell. *Bioresour. Technol. Rep.* **2021**, *15*, No. 100785.
(41) Parmar, K. Biomass- An Overview on Composition Characteristics and Properties. *IRA-International J. Appl. Sci. (ISSN 2455-4499)* **2017**, *7*, 42.
(42) Salaheldeen, M.; Aroua, M. K.; Mariod, A. A.; Cheng, S. F.; Abdelrahman, M. A. An Evaluation of Moringa Peregrina Seeds as a Source for Bio-Fuel. *Ind. Crops Prod.* **2014**, *61*, 49−61.
(43) Volli, V.; Singh, R. K. Production of Bio-Oil from de-Oiled Cakes by Thermal Pyrolysis. *Fuel* **2012**, *96*, 579−585.
(44) Rapagnà, S.; Jand, N.; Kiennemann, A.; Foscolo, P. U. Steam-Gasification of Biomass in a Fluidised-Bed of Olivine Particles. *Biomass and Bioenergy* **2000**, *19*, 187−197.
(45) Li, B.; Yang, H.; Wei, L.; Shao, J.; Wang, X.; Chen, H. Hydrogen Production from Agricultural Biomass Wastes Gasification in a Fluidized Bed with Calcium Oxide Enhancing. *Int. J. Hydrogen Energy* **2017**, *42*, 4832−4839.
(46) Hantoko, D.; Antoni; Kanchanatip, E.; Yan, M.; Weng, Z.; Gao, Z.; Zhong, Y. Assessment of Sewage Sludge Gasification in Supercritical Water for H 2 -Rich Syngas Production. *Process Saf. Environ. Prot.* **2019**, *131*, 63−72.

https://doi.org/10.1021/acsomega.3c00908
ACS Omega 2023, 8, 13396−13409